**Supplementary Information**

**General methods:**

Unless otherwise stated, all reagents were obtained from commercial suppliers and were used without further purification. Flash column chromatography was performed with silica gel (230-400 mesh). TLC was performed on pre-coated silica plates and visualized using UV light and by applying a solution of 10% ammonium molybdate in 2M $H_2SO_4$ followed by heating. Moisture sensitive reactions were carried out under an atmosphere of dry nitrogen. $CH_3CN$ was distilled over $CaH_2$. Methanol was distilled over magnesium and iodine. THF was distilled over sodium/benzophenone. All NMR spectra were acquired on Bruker AV-400 or Bruker AV-600 spectrometers at 25 ºC. Chemical shifts are reported in ppm (δ) relative to tetramethylsilane ($^1$H-NMR) or $CDCl_3$ ($^{13}$C-NMR). NMR spectra of thioamide-containing compounds were difficult to interpret due to the presence of multiple stable rotamers.

**Synthesis:**

**3,4,6-tri-*O*-acetyl-2-*N*-acetamido-D-glucal (6)**:

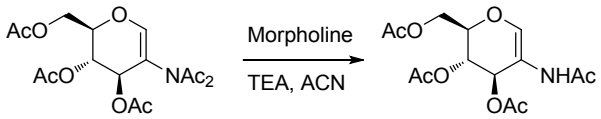


**(6)**

A solution of the acetimide[1] (224 mg, 0.6 mmol) in dry acetonitrile (3 mL, 5 mL/mmol), was treated with TEA (0.4 mL, 3.0 mmol) and morpholine (0.16 mL, 1.8 mmol) under nitrogen and the resulting mixture was stirred at r.t. for 28 h, after which the solvent was evaporated. The crude material was purified by silica column chromatography (PE/EA 4:6 to 1:9), affording the title compound (174 mg, 88%) as a white foam.

**$^1$H-NMR** ($CDCl_3$, 400 MHz): 1.97 (3H, s, OAc), 2.05 (6H, s, 2x OAc), 2.06 (3H, s, NHAc), 4.18 (1H, dd, *J* = 2.4, 10.7 Hz, H-6a), 4.28-4.38 (2H, m, H-5, 6b), 5.16 (1H, dd, *J* = 4.1, 4.6 Hz, H-4), 5.28 (1H, d, *J* = 4.1 Hz, H-3), 6.94 (1H, br s, H-NHAc), 7.33 (1H, s, H-1). **$^{13}$C-NMR** ($CDCl_3$, 100 MHz): 20.6 (OAc), 20.7 (OAc), 20.8 (OAc), 23.6 (NHAc), 61.0 ($CH_2$, C-6), 67.0 (CH, C-4), 67.2 (CH, C-3), 73.1 (CH, C-5), 111.1 (C, C-2), 140.2 (CH, C-1), 168.8 (CO, OAc), 169.5 (CO, OAc), 170.4 (CO, OAc), 171.5 (CO, NHAc).
**LRMS** (pos): m/z 352.3 $[M+Na]^+$. **HRMS**: calcd for $C_{14}H_{19}NO_8Na$: 352.1008; found: 352.1013.

**3,4,6-tri-*O*-acetyl-2-*N*-thioacetamido-D-glucal (7):**

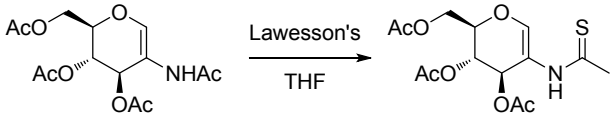


**(6)** **(7)**

[1] N. Pravić, I. Franjic-Mihalic, B. Danilov, *Carbohydr. Res.* **1975**, *45*, 302 – 306.

A solution of the *N*-acetyl-glycal (120 mg, 0.365 mmol) in dry THF (5.5 mL, 15 mL/mmol) was treated with Lawesson's reagent (118 mg, 0.292 mmol) and the resulting mixture was stirred under nitrogen for 22 h, after which the solvent was evaporated. Flash column chromatography of the crude material (Tol/EA 7:3 to 1:1) afforded the desired thio-amide (60 mg, 48%) as a colorless oil.

$^{1}$H-NMR/$^{13}$C-NMR: Mixture of conformers/rotamers in a 2:1 ratio. Selected **$^{1}$H-NMR** ($CDCl_3$, 400 MHz) signals for major compound: 2.54 (3H, s, NH(C=S)$CH_3$), 7.60 (1H, s, H-1), 8.36 (1H, br.s, H-NH). Selected **$^{13}$C-NMR** ($CDCl_3$, 100 MHz) signals for major compound: 35.1 ($CH_3$, NH(C=S)$CH_3$), 113.2 (C, C-2), 144.6 (CH, C-1), 201.6 (C, C=S).
**LRMS** (pos): m/z 368.3 $[M+Na]^+$. **HRMS**: calcd for $C_{14}H_{19}NO_7SNa$: 368.0780; found: 368.0776.

**2-*N*-thioacetamido-D-glucal (5):**

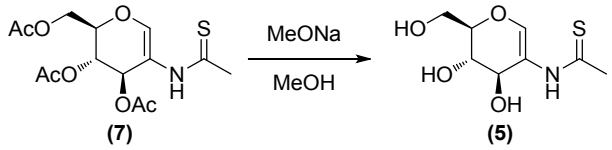


A solution of the thioamide **7** (26 mg, 0.075 mmol) in dry MeOH (2.0 mL, 25 mL/mmol) was cooled down with an ice bath and subsequently treated with a catalytic amount of sodium; the resulting mixture was stirred under nitrogen for 2 h, after which a scoop of silica was added and the solvent evaporated. Flash column chromatography of the crude material (DCM/MeOH 5% to 10%) afforded the deprotected product **5** as a colorless oil that was redissolved in deionized water and freeze-dried overnight to afford a pale yellow foam (10 mg, 61%).

**$^{1}$H-NMR** (MeOD, 400 MHz): 2.54 (3H, s, NH(S=C)$CH_3$), 3.73 (1H, dd, *J* = 6.5, 8.8Hz, H-4), 3.85 (1H, d, *J* = 5.6Hz, H-6a), 3.86 (1H, d, *J* = 3.3, H-6b), 3.92 (1H, m, H-5), 4.57 (1H, d, *J* = 6.5Hz, H-3), 6.93 (1H, s, H-1). **$^{13}$C-NMR** (MeOD, 100 MHz): 33.8 ($CH_3$, NH(C=S)$CH_3$), 62.1 ($CH_2$, C-6), 70.1 (CH, C-3), 70.6 (CH, C-4), 81.1 (CH, C-5), 119.2 (C, C-2), 144.0 (CH, C-1), 203.8 (C, C=S).
**LRMS** (pos): m/z 242.4 $[M+Na]^+$. **HRMS**: calcd for $C_8H_{13}NO_4SNa$: 242.0463; found: 242.0464.

**Acetyl Chitobial (8):**

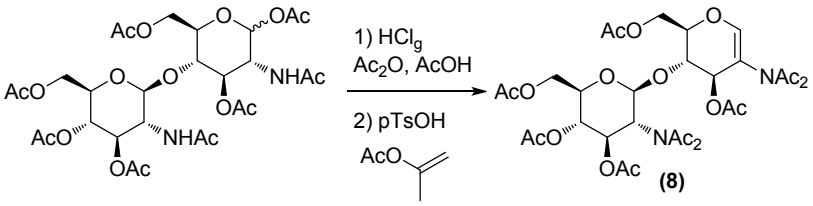


To a suspension of acetyl chitobiose (1 g, 1.48 mmol) in acetic anhydride (10 mL, 6.5 mL/mmol) acetic acid (aprox 1.5 mL) was added dropwise until the solution was clear and then cooled with an ice bath. Hydrogen chloride gas was bubbled gently through this solution for 15 min and the resulting mixture

was stirred at r.t. for 5 days, after which the solvents were evaporated. The resulting crude material was extracted with ethyl acetate (twice) and washed with ice-cold water, then with saturated sodium bicarbonate solution and brine. The combined organic phase was dried over anhydrous sodium sulfate and evaporated under vacuum to yield 620 mg (64%) of crude peracetylated chitobiosyl chloride. This material was used in the next step without further purification.

A solution of the crude chloride (620 mg, 0.95 mmol) in isopropenyl acetate (12 mL, 12 mL/mmol) was treated with *p*-toluensulfonic acid hydrate (1.8 mg, 0.01 mmol) and the resulting mixture was refluxed under inert atmosphere for 18 h, after which the solvent was evaporated. Silica column chromatography (PE/EA 50% to 100%) afforded the desired peracetylated glycal (**8**) (280 mg, 42%) as a colorless oil.

**$^1$H-NMR** ($CDCl_3$, 400 MHz): 1.97 (3H, s, OAc), 2.00 (6H, s, 2x OAc), 2.06 (3H, s, OAc), 2.10 (3H, s, OAc), 2.32 (12H, s, 2x $NAc_2$), 3.71 (1H, dd, *J* = 7.8, 10.3 Hz, H-2'), 3.75-3.81 (1H, m, H-5'), 4.03-4.09 (2H, m, H-4, 6a), 4.18-4.38 (4H, m, H-5, 6b, 6'a, 6'b), 5.07 (1H, t, *J* = 9.5 Hz, H-4'), 5.54 (1H, d, *J* = 7.8 Hz, H-1'), 5.59 (1H, d, *J* = 4.4 Hz, H-3), 5.76 (1H, t, *J* = 9.0 Hz, H-3'), 6.50 (1H, s, H-1). **$^{13}$C-NMR** ($CDCl_3$, 100 MHz): 20.4 (OAc), 20.54 (OAc), 20.58 (OAc), 20.60 (OAc), 20.7 (OAc), 24.9 ($NAc_2$), 27.5 ($NAc_2$), 60.9, 61.6, 62.0, 67.3, 68.9, 70.0, 71.6, 73.1, 74.6, 98.4 (CH, C-1'), 112.8 (C, C-2), 147.6 (CH, C-1), 169.55, 169.57, 169.62, 170.2, 170.5, 174.0 (CO, $NAc_2$), 175.1 (CO, $NAc_2$).
**LRMS** (pos): m/z 723.4 $[M+Na]^+$. **HRMS**: calcd for $C_{30}H_{40}N_2O_{17}Na$: 723.2225; found: 723.2241.

**Chitobial (9):**

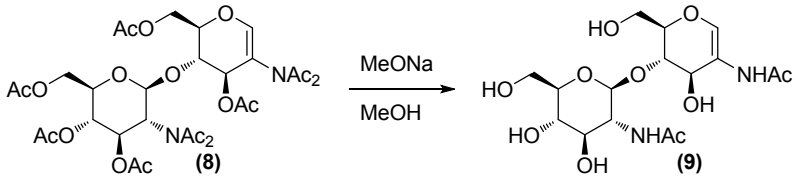


A solution of the acetylated chitobial (138 mg, 0.197 mmol) in dry MeOH (5.0 mL, 25 mL/mmol) was cooled down with an ice bath and subsequently treated with a catalytic amount of sodium; the resulting mixture was stirred under nitrogen for 2 h, after which a scoop of silica was added and the solvent evaporated. Flash column chromatography of the crude material (EA/MeOH/$H_2O$ 9:2:1) afforded the deprotected product **9** as a colorless oil that was redissolved in deionized water and freeze-dried overnight to afford a pale yellow foam (62 mg, 78%).

**$^1$H-NMR** (MeOD, 400 MHz): 1.90 (6H, brs, 2x NHAc), 3.29 (1H, dd, *J* = 9.4, 9.6 Hz, H-4'), 3.37 (1H, ddd, *J* = 2.0, 7.2, 9.6 Hz, H-5'), 3.47 (1H, t, *J* = 9.4 Hz, H-3'), 3.63 (1H, dd, *J* = 7.2, 11.6 Hz, H-6'a), 3.71 (1H, dd, *J* = 8.4, 9.9 Hz, H-2'), 3.72-3.88 (4H, m, H-4, 5, 6a, 6b), 3.94 (1H, dd, *J* = 2.0, 11.6 Hz, H-6'b), 4.36 (1H, d, *J* = 5.5 Hz, H-3), 4.58 (1H, d, *J* = 8.4 Hz, H-1'), 6.95 (1H, s, H-1). **$^{13}$C-NMR** (MeOD, 100 MHz): 23.0 (NHAc), 23.1 (NHAc), 57.5 (CH, C-2'), 61.4 ($CH_2$, C-6), 62.9 ($CH_2$, C-6'), 69.9 (CH, C-3), 72.4 (CH, C-4'), 76.0 (CH, C-3'), 78.2 (CH, C-5'), 78.6 (CH, C-4/5), 79.9 (CH, C-5/4), 103.2 (CH, C-1'), 116.0 (C, C-2), 140.6 (CH, C-1), 172.8 (CO, NHAc), 173.9 (CO, NHAc).
**LRMS** (pos): m/z 429.3 $[M+Na]^+$. **HRMS**: calcd for $C_{16}H_{26}N_2O_{10}Na$: 429.1485; found: 429.1489.

**GalNAc-chitobial (10):**

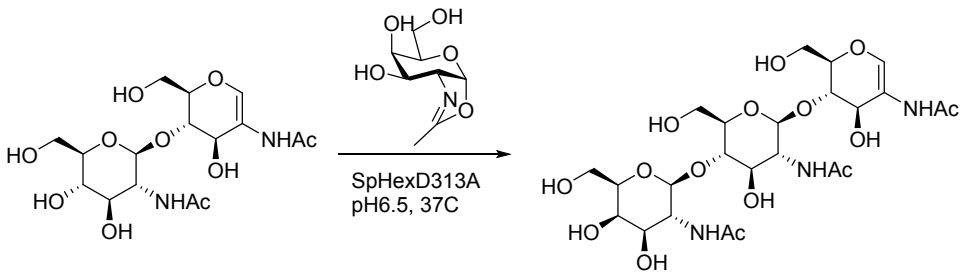


Chitobial (**9**) (11 mg, 0.027 mmol) and GalNAc-oxazoline[2] (25 mg, 0.123 mmol) were dissolved in 0.8 mL buffer (25mM sodium phosphate, 25mM sodium citrate, 100mM sodium chloride, pH6.5) and subsequently treated with SpHexD313A (0.2 mL, 0.9 mg/mL). The resulting mixture was incubated at 37 °C overnight. Flash column chromatography of the crude material (EA/MeOH/$H_2O$ 15:2:1 to 5:2:1) followed by C18 size-exclusion chromatography afforded the desired product (**10**) as a colorless oil, along with 7.0 mg of recovered starting material. The trisaccharide was redissolved in deionized water and freeze-dried overnight to afford a pale yellow foam (3.7 mg, 22%, 62% brsm).

**$^1$H-NMR** ($D_2O$, 600 MHz): 2.06 (3H, s, NHAc), 2.07 (3H, s, NHAc), 2.08 (3H, s, NHAc), 3.58 (1H, ddd, *J* = 2.0, 5.8, 9.7 Hz), 3.66 (1H, dd, *J* = 8.2, 9.6 Hz), 3.68 (1H, dd, *J* = 3.7, 6.3 Hz), 3.72-3.84 (8H, m), 3.87 (1H, dd, *J* = 2.0, 12.0 Hz), 3.91-3.95 (2H, m), 3.96 (1H, d, *J* = 2.6 Hz), 4.08 (1H, ddd, *J* = 4.1, 4.1, 7.8 Hz), 4.40 (1H, d, *J* = 5.6 Hz), 4.53 (1H, d, *J* = 8.5 Hz), 4.69 (1H, d, *J* = 8.2 Hz), 6.76 (1H, s). **$^{13}$C-NMR** ($D_2O$, 151 MHz): 24.5 (NHAc), 24.6 (NHAc), 24.7 (NHAc), 55.1 (CH), 57.5 (CH), 62.0 ($CH_2$), 62.7 ($CH_2$), 63.6 ($CH_2$), 69.8 (CH), 70.3 (CH), 73.3 (CH), 74.8 (CH), 77.1 (CH), 77.9 (CH), 79.5 (CH), 79.8 (CH), 81.7 (CH), 103.6 (CH), 104.4 (CH), 112.6 (C), 141.3 (CH), 174.4 (CO, NHAc), 174.6 (CO, NHAc), 174.7 (CO, NHAc).
**LRMS** (pos): m/z 632.4 $[M+Na]^+$. **HRMS**: calcd for $C_{24}H_{39}N_3O_{15}Na$: 632.2279; found: 632.2280.

[2] M. Noguchi, T. Tanaka, H. Gyakushi, A. Kobayashi, S.-i. Shoda, *J. Org. Chem*. **2009**, *74*, 2210 – 2212.

**Inhibition Kinetics:**

Kinetic studies were performed at 25 °C in 25mM sodium citrate, 25mM sodium phosphate, 100mM sodium chloride buffer in the presence of 1% BSA either at pH5 or pH7, using a known concentration of enzyme (SpHexWT = $2.1x10^{-7}$mM; SpHexD313A = $2.85x10^{-5}$mM; SpHexE314Q = $5.35x10^{-5}$mM). The enzyme was incubated with different concentrations of the inhibitors for 2-5 minutes before initiating the reaction by the addition of substrate and the initial rate was measured by monitoring the increase in absorbance at 400 nm (pH7, $\varepsilon$ = 10587 $M^{-1}cm^{-1}$) or at 348 nm (pNP isosbestic point, pH5-6, $\varepsilon$ = 6700 $M^{-1}cm^{-1}$) for up to ten minutes. $K_i$ determinations were performed using two to four different substrate concentrations. For each inhibitor, a range of four to six inhibitor concentrations bracketing the $K_i$ value was used for each substrate concentration. Dixon plots (1/v vs [I]) were constructed to validate the use of competitive inhibition model and to assess the fit of the rest of the data. A competitive inhibition model was fit to the data by using non-linear regression analysis with Grafit 7.0.[3]

## Dixon plots pH5

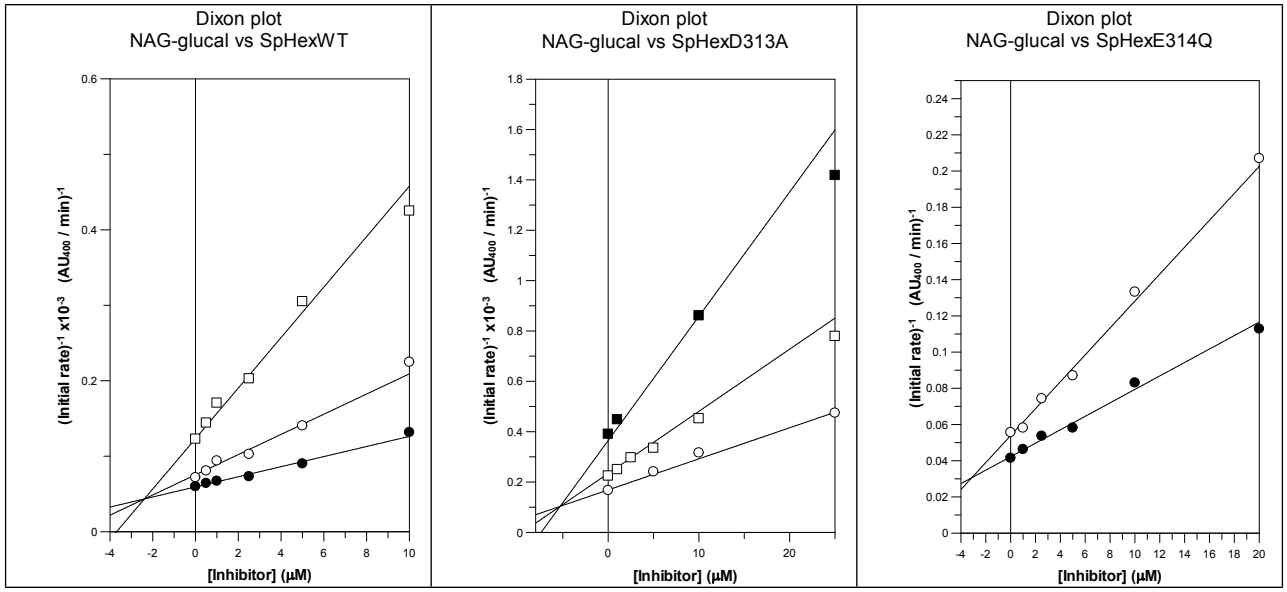


[3] Leatherbarrow, R.J. (2010) GraFit Version 7, Erithacus Software Ltd., Horley, U.K.

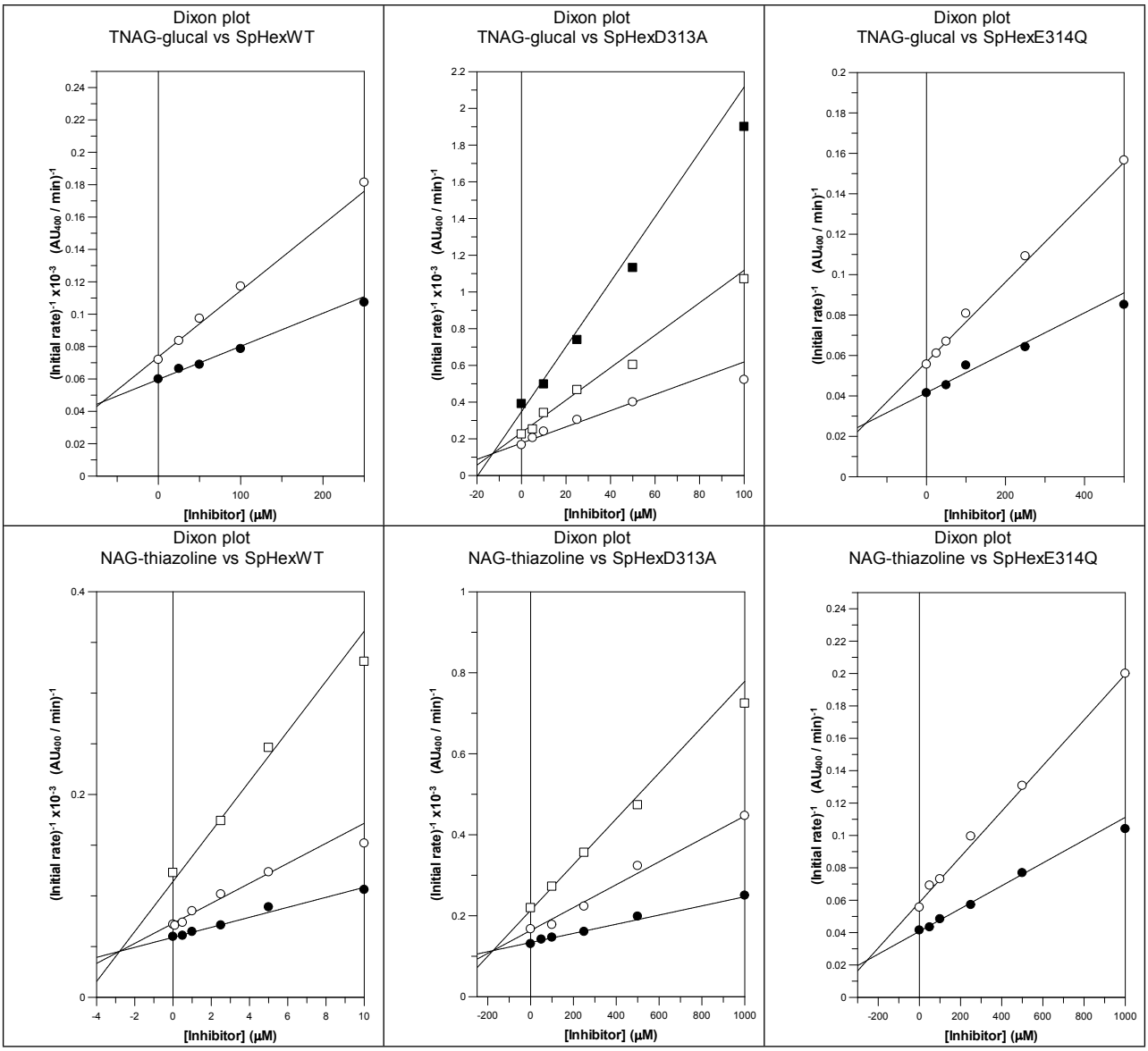
Dixon plot
TNAG-glucal vs SpHexWT
(Initial rate)-1 x10-3 (AU400 / min)-1
[Inhibitor] (µM)
Dixon plot
TNAG-glucal vs SpHexD313A
(Initial rate)-1 x10-3 (AU400 / min)-1
[Inhibitor] (µM)
Dixon plot
TNAG-glucal vs SpHexE314Q
(Initial rate)-1 (AU400 / min)-1
[Inhibitor] (µM)
Dixon plot
NAG-thiazoline vs SpHexWT
(Initial rate)-1 x10-3 (AU400 / min)-1
[Inhibitor] (µM)
Dixon plot
NAG-thiazoline vs SpHexD313A
(Initial rate)-1 x10-3 (AU400 / min)-1
[Inhibitor] (µM)
Dixon plot
NAG-thiazoline vs SpHexE314Q
(Initial rate)-1 (AU400 / min)-1
[Inhibitor] (µM)

## Dixon plots pH7

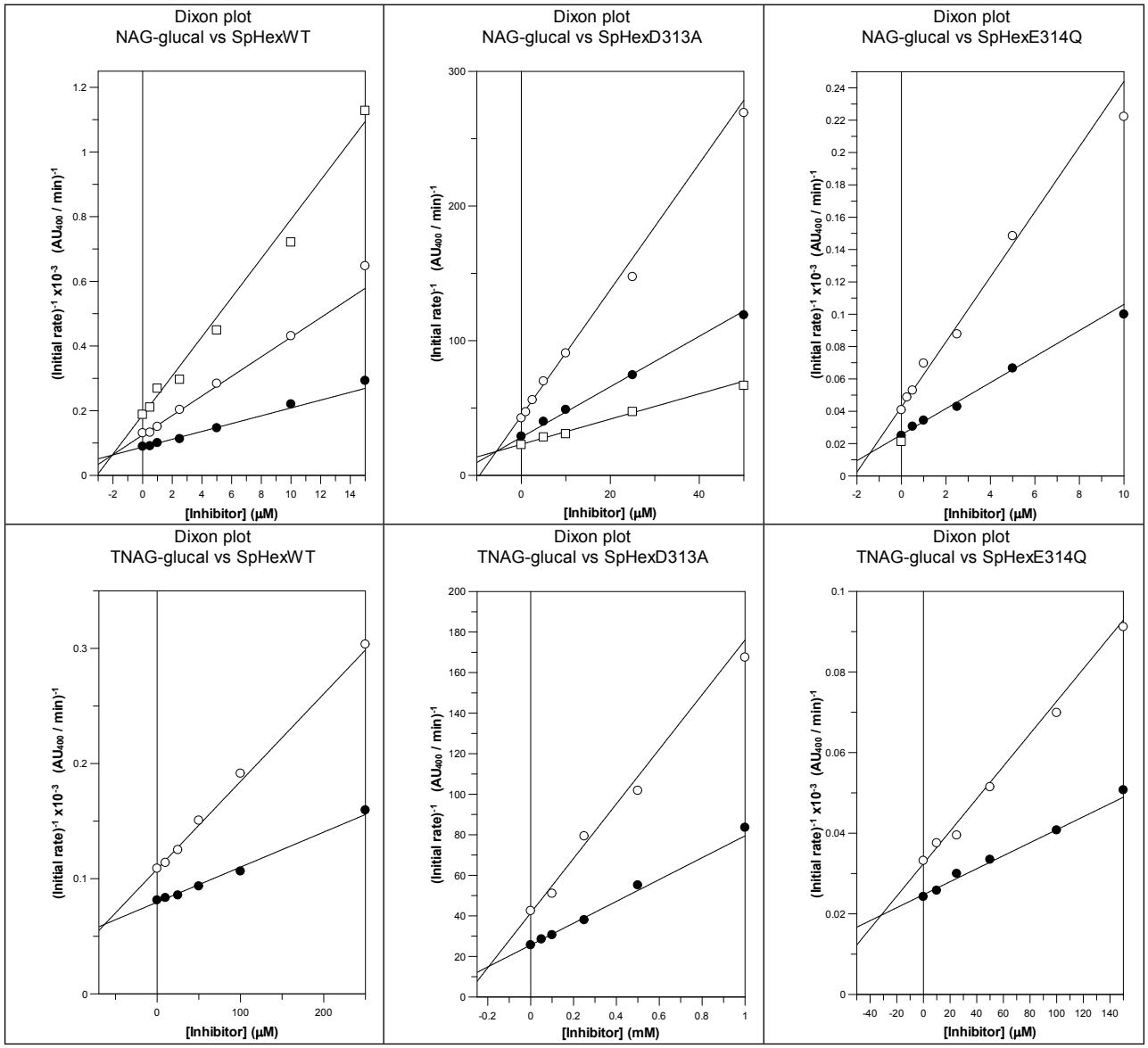

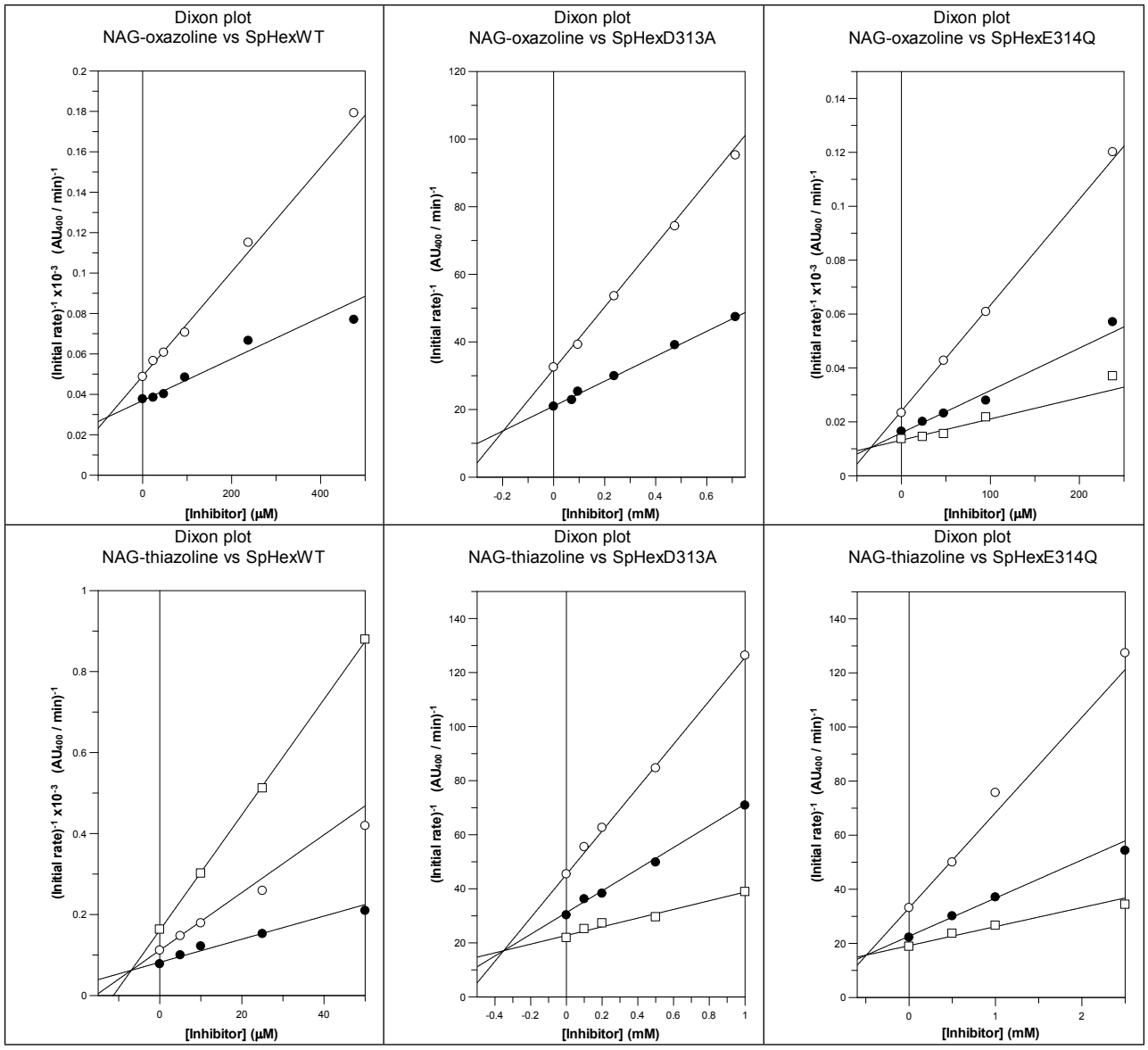
Dixon plot
NAG-oxazoline vs SpHexWT
(Initial rate)-1 x10-3 (AU400 / min)-1
[Inhibitor] (µM)
Dixon plot
NAG-oxazoline vs SpHexD313A
(Initial rate)-1 (AU400 / min)-1
[Inhibitor] (mM)
Dixon plot
NAG-oxazoline vs SpHexE314Q
(Initial rate)-1 x10-3 (AU400 / min)-1
[Inhibitor] (µM)
Dixon plot
NAG-thiazoline vs SpHexWT
(Initial rate)-1 x10-3 (AU400 / min)-1
[Inhibitor] (µM)
Dixon plot
NAG-thiazoline vs SpHexD313A
(Initial rate)-1 (AU400 / min)-1
[Inhibitor] (mM)
Dixon plot
NAG-thiazoline vs SpHexE314Q
(Initial rate)-1 (AU400 / min)-1
[Inhibitor] (mM)

## Michaelis-Menten plots for NAG-pNP (pH5):

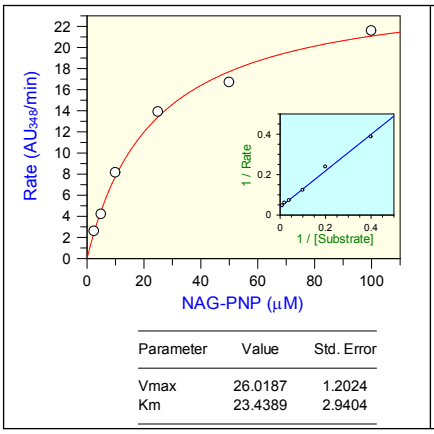


| Parameter | Value | Std. Error |
|---|---|---|
| Vmax | 26.0187 | 1.2024 |
| Km | 23.4389 | 2.9404 |

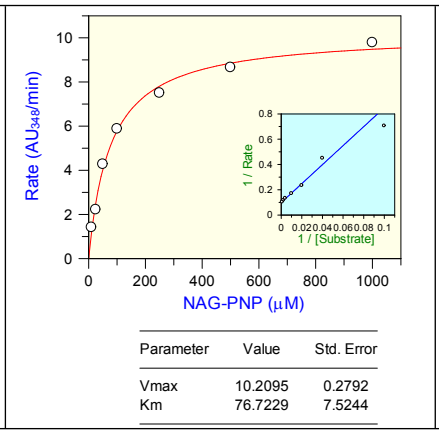


| Parameter | Value | Std. Error |
|---|---|---|
| Vmax | 10.2095 | 0.2792 |
| Km | 76.7229 | 7.5244 |

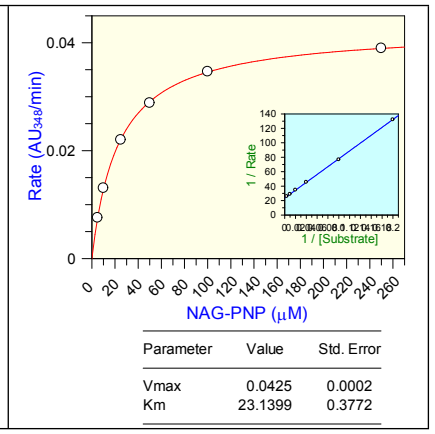


| Parameter | Value | Std. Error |
|---|---|---|
| Vmax | 0.0425 | 0.0002 |
| Km | 23.1399 | 0.3772 |

## Michaelis-Menten plots for NAG-pNP (pH7):

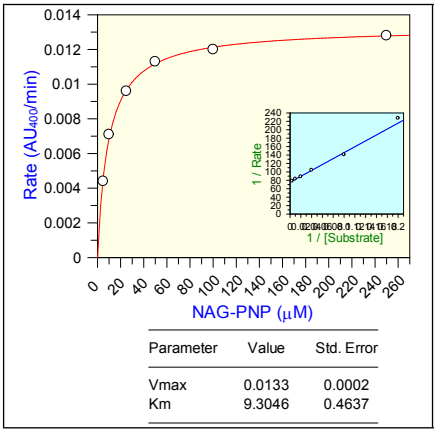


| Parameter | Value | Std. Error |
|---|---|---|
| Vmax | 0.0133 | 0.0002 |
| Km | 9.3046 | 0.4637 |

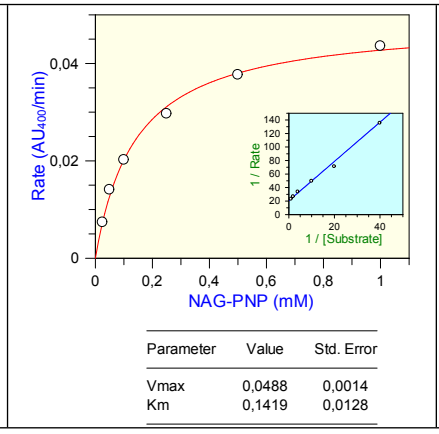


| Parameter | Value | Std. Error |
|---|---|---|
| Vmax | 0,0488 | 0,0014 |
| Km | 0,1419 | 0,0128 |

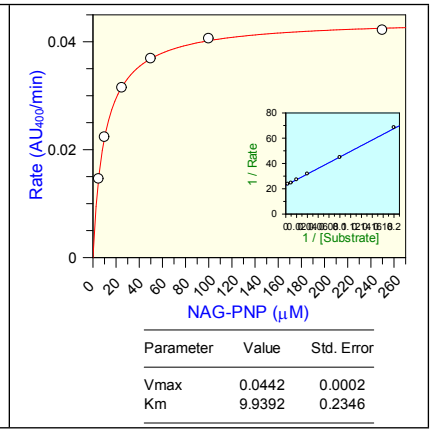


| Parameter | Value | Std. Error |
|---|---|---|
| Vmax | 0.0442 | 0.0002 |
| Km | 9.9392 | 0.2346 |

**Michaelis-Menten plot for NA-glucal hydration:**

The initial rates of a series of reactions with varying substrate concentrations were measured by monitoring the disappearance of the absorbance at 250nm (due to the double bond, $\varepsilon$ = 1246.4 $M^{-1}cm^{-1}$) in 25mM sodium citrate, 25mM sodium phosphate, 100mM sodium chloride buffer containing 0.1% BSA at 25 °C with a final enzyme concentration of 4.2 μM. The reaction rates thus obtained were plotted against their corresponding initial substrate concentration, and fitted to the Michaelis-Menten equation modified for substrate inhibition:

$$v = \frac{Vmax[S]}{Km + [S] + \frac{[S]^2}{Ki}}$$

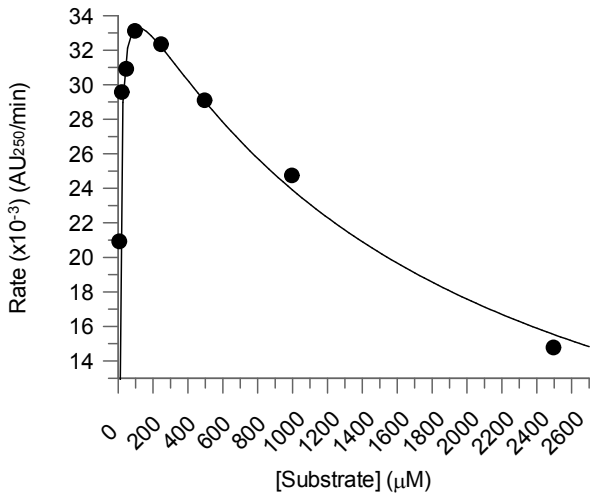


**Vmax = 0.03 mM/min**
**$k_{cat}$ = 0.12 $s^{-1}$**
**$K_m$ = 7.8 ± 0.8 (μM)**
**$K_i$ = 1751 ± 164 (μM)**

**Chitinases: Dixon plots**

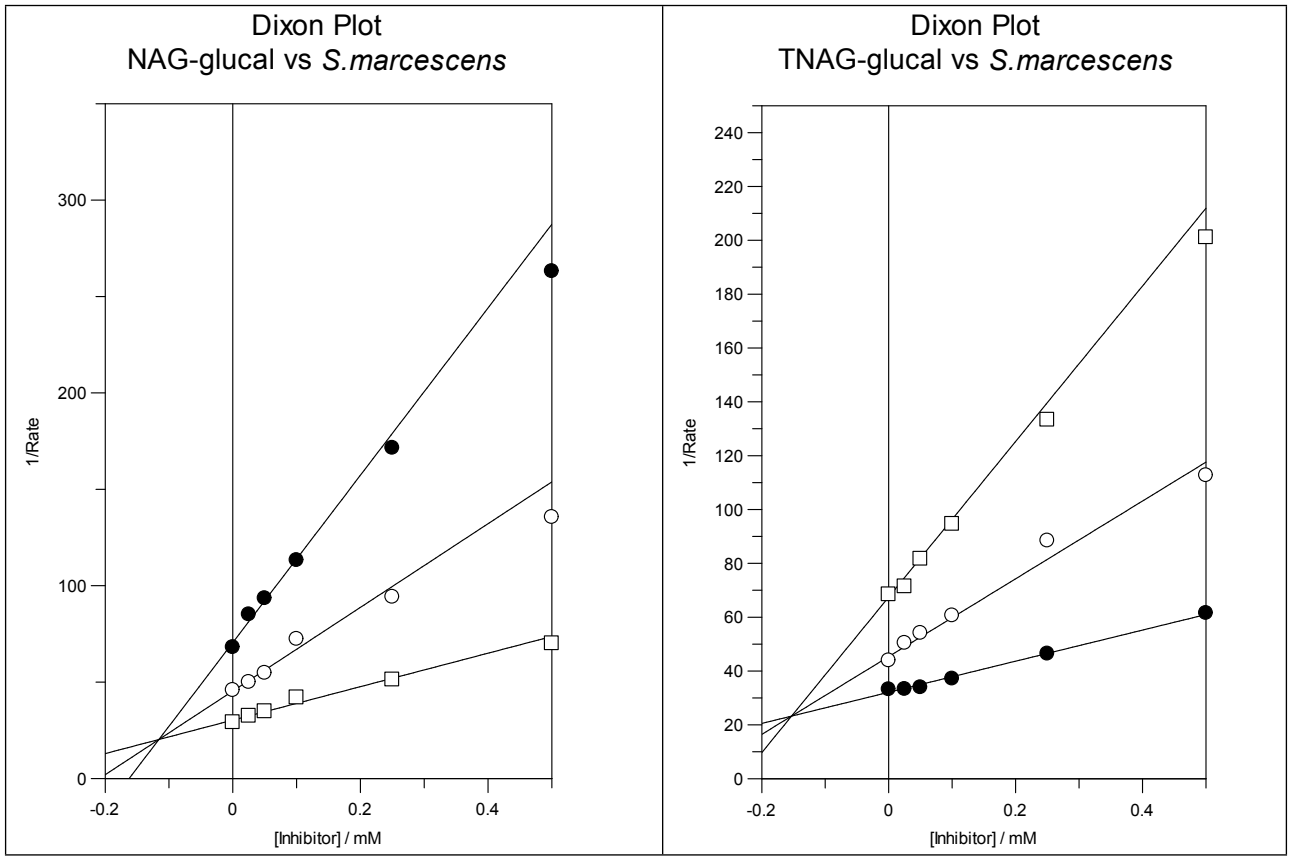

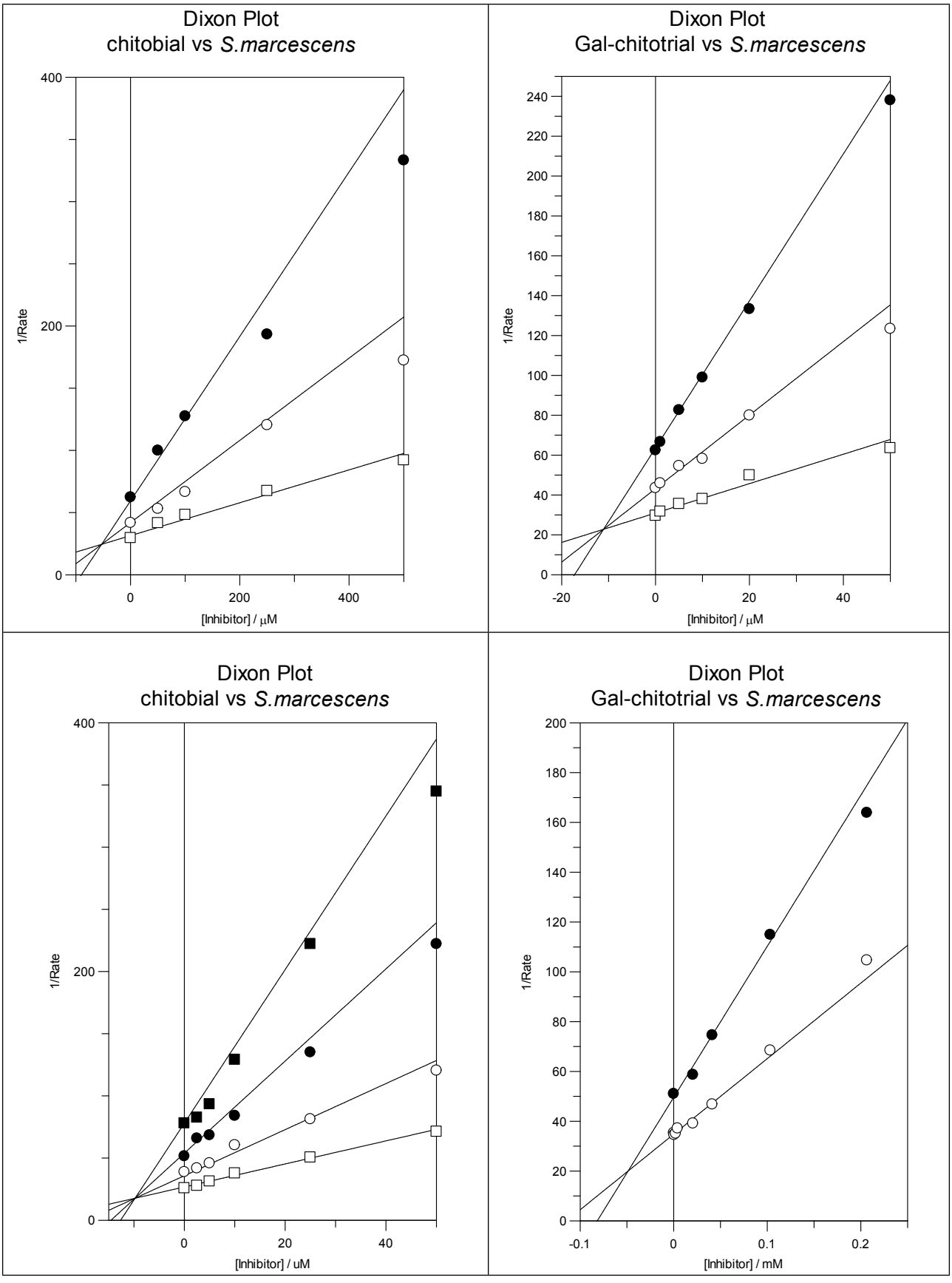
Dixon Plot
chitobial vs S.marcescens
1/Rate
[Inhibitor] / μM
Dixon Plot
Gal-chitotrial vs S.marcescens
1/Rate
[Inhibitor] / μM
Dixon Plot
chitobial vs S.marcescens
1/Rate
[Inhibitor] / uM
Dixon Plot
Gal-chitotrial vs S.marcescens
1/Rate
[Inhibitor] / mM

**Crystallography:**

**Table S1: Crystallographic and refinement statistics for *Sp*HEX bound to NTA-glucal and NA-glucal.**

| **Data collection** | ***Sp*HEX NTA-glucal** | ***Sp*HEX NA-glucal** |
|---|---|---|
| **Space group** | P $6_1$ 2 2 | P $6_1$ 2 2 |
| **Unit cell dimensions** | $a = b = 133.87$ Å, $c = 174.91$ Å | $a = b = 133.17$ Å, $c = 176.52$ Å |
| **Resolution (Å)** | 62.51 - 2.45 (2.55 - 2.45)* | 54.81 - 2.00 (2.05 - 2.00) |
| **$R_{merge}$** | 0.135 (0.544) | 0.123 (0.704) |
| **CC(1/2)** | 0.990 (0.867) | 0.995 (0.772) |
| **I / σI** | 12.4 (3.4) | 11.1 (2.3) |
| **Completeness (%)** | 96.7 (96.0) | 98.2 (94.1) |
| **Redundancy** | 9.0 (8.7) | 7.2 (6.6) |
| **Refinement** | | |
| $R_{work}$ / $R_{free}$ | 0.15 / 0.21 | 0.15 / 0.18 |
| **B-factor (Å$^2$)** | 29.54 | 25.39 |
| Protein | 29.20 | 23.28 |
| Ligands | 39.21 | 35.70 |
| Solvent | 32.11 | 36.96 |
| **R.m.s. deviations** | | |
| Bond lengths (Å) | 0.012 | 0.011 |
| Bond angles (°) | 1.15 | 1.06 |
| **Ramachandran plot** favoured/allowed (%) | 98/ 1.8 | 99/ 1.4 |

* Values in parentheses refer to the high-resolution shell.

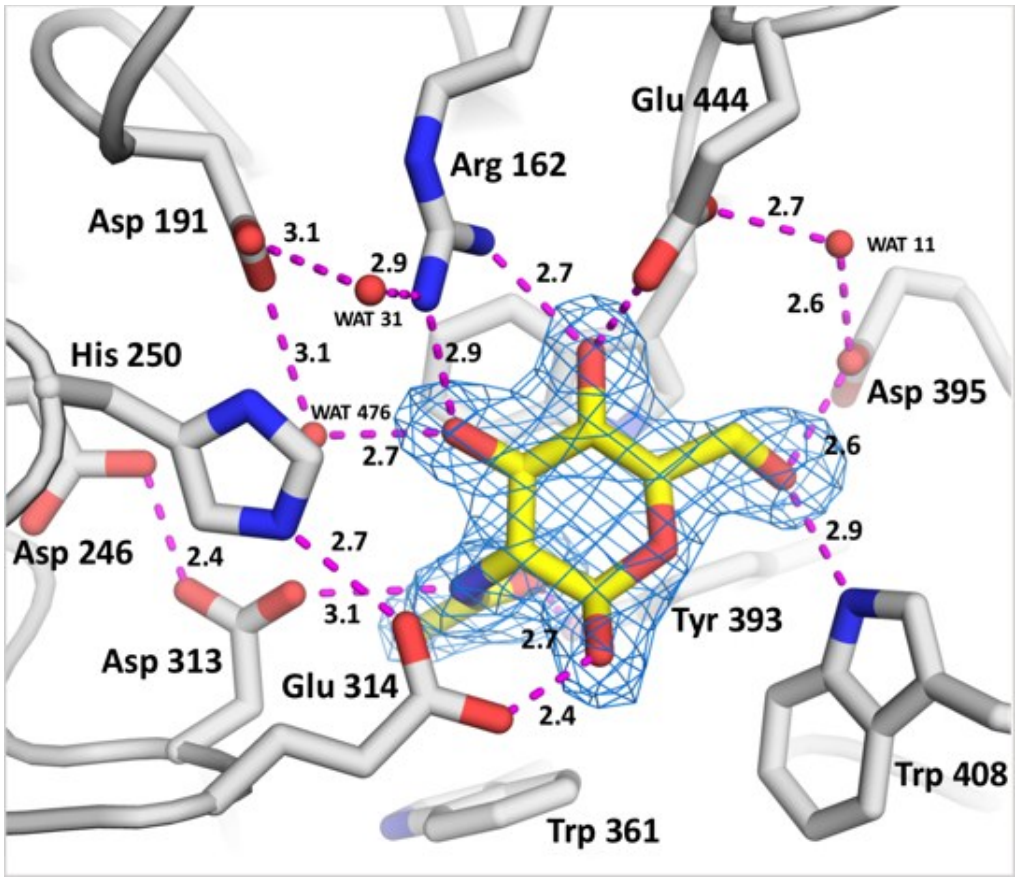


**Figure S1.** GlcNAc bound to *SpHex*. Active site residues (grey) and GlcNAc (yellow) are drawn as sticks. Oxygen and nitrogen atoms are coloured red and blue, respectively. Red spheres represent waters. Hydrogen-bonds are shown by dashed lines. Electron density is an $|F_o|-|F_c|$ omit map contoured at 5.0 rmsd.

NMR spectra:

AGS thio-GlcNAc-glycal.001.001.1r.esp

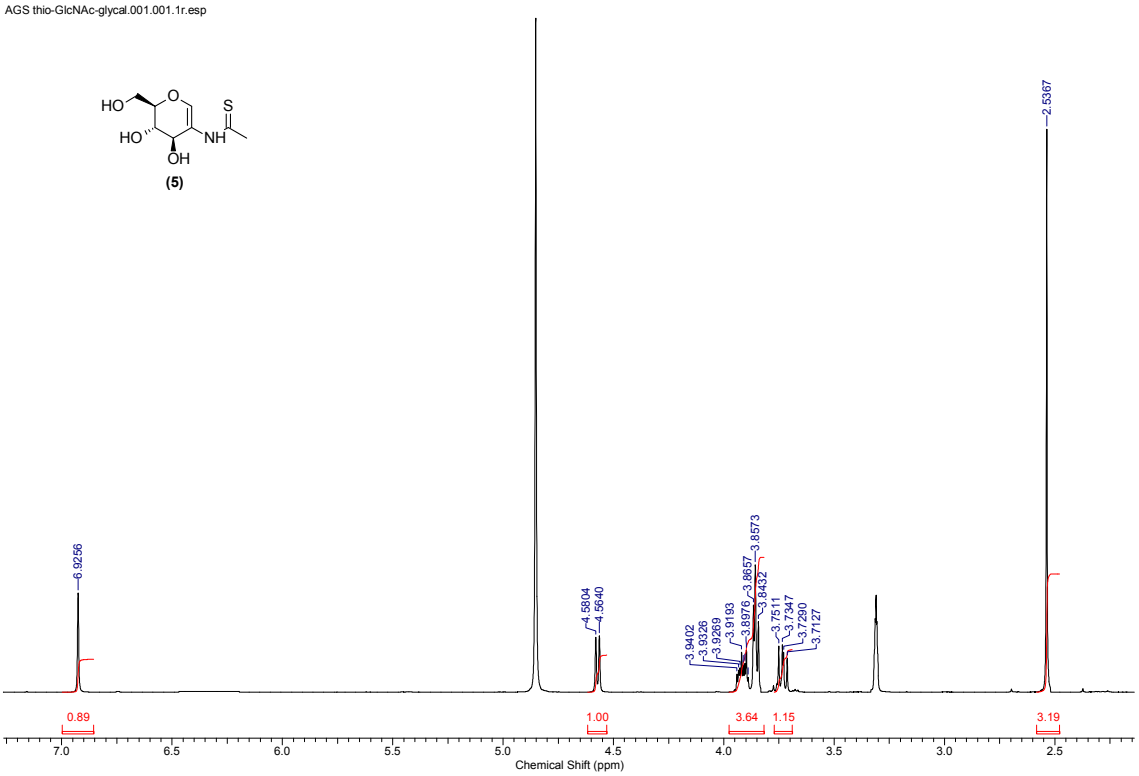


AGS thio-GlcNAc-glycal.003.001.1r.esp

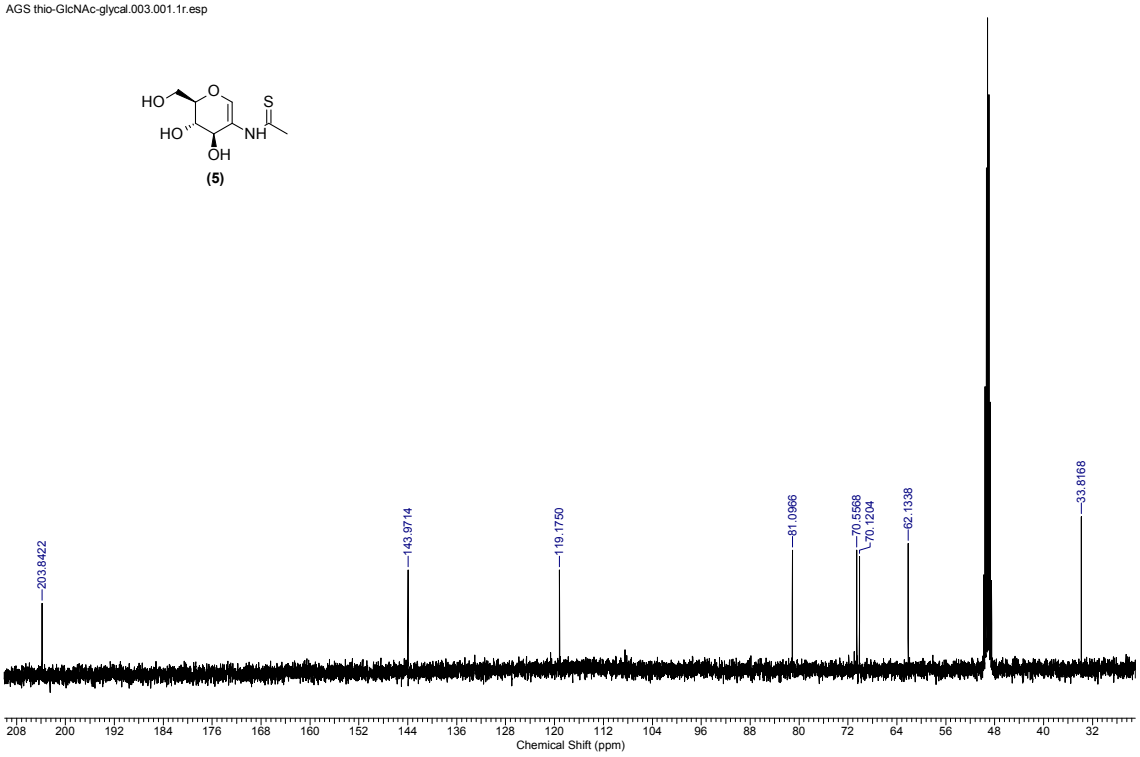

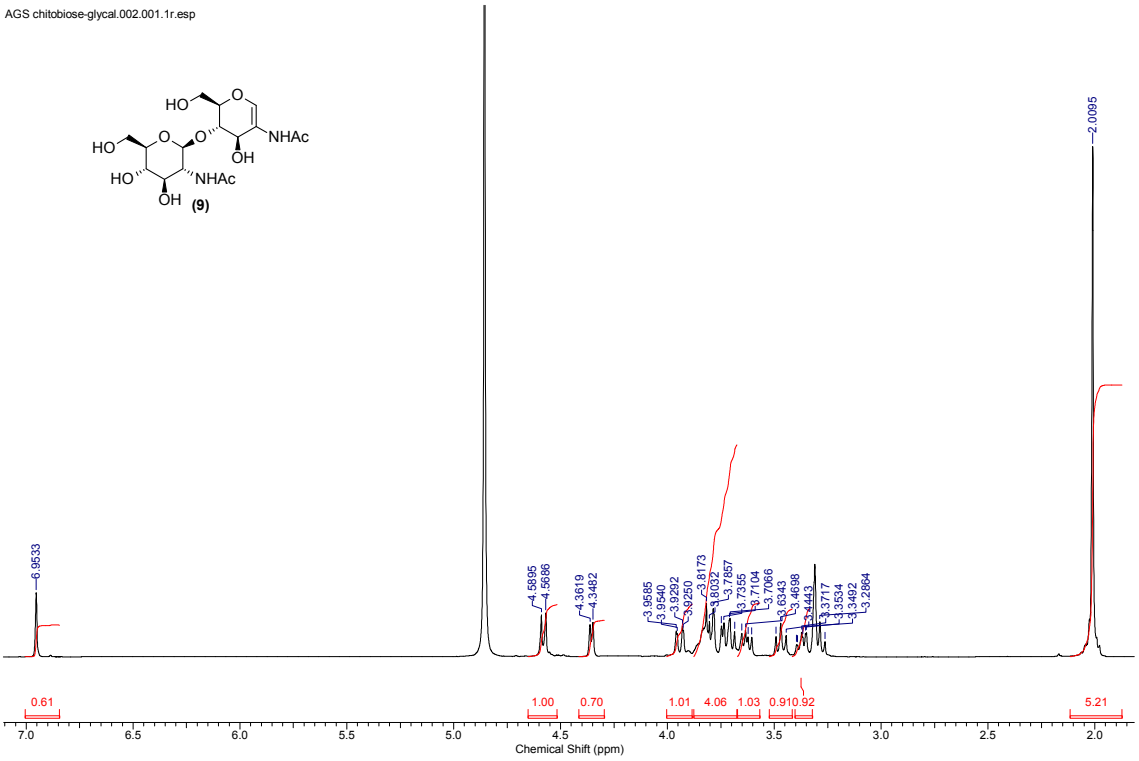
AGS chitobiose-glycal.002.001.1r.esp
HO
O
NHAc
OH
HO
O
O
HO
NHAc
OH
(9)
6.9533
4.5895
4.5686
4.3619
4.3482
3.9585
3.9540
3.9292
3.9250
3.8173
3.8032
3.7857
3.7355
3.7104
3.7066
3.6343
3.4698
3.4443
3.3717
3.3534
3.3492
3.2864
2.0095
0.61
1.00
0.70
1.01
4.06
1.03
0.91
0.92
5.21
Chemical Shift (ppm)

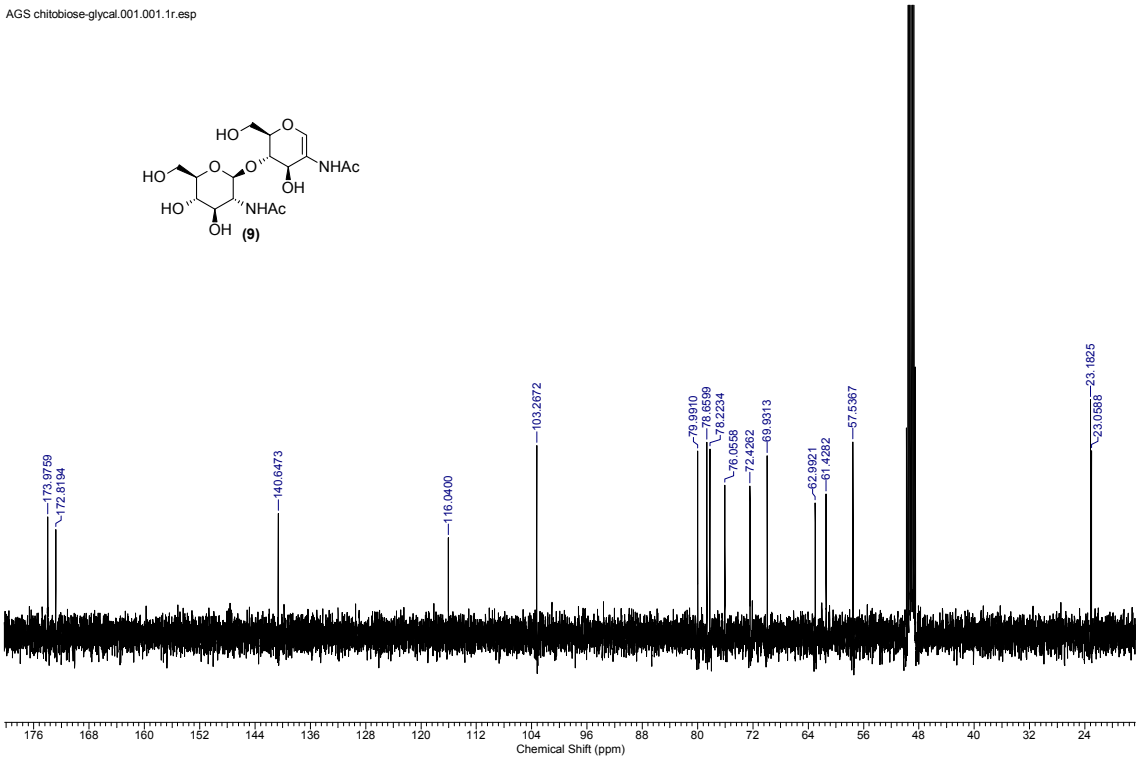
AGS chitobiose-glycal.001.001.1r.esp
HO
O
NHAc
OH
HO
O
O
HO
NHAc
OH
(9)
173.9759
172.8194
140.6473
116.0400
103.2672
79.9910
78.6599
78.2234
76.0558
72.4262
69.9313
62.9921
61.4282
57.5367
23.1625
23.0588
Chemical Shift (ppm)

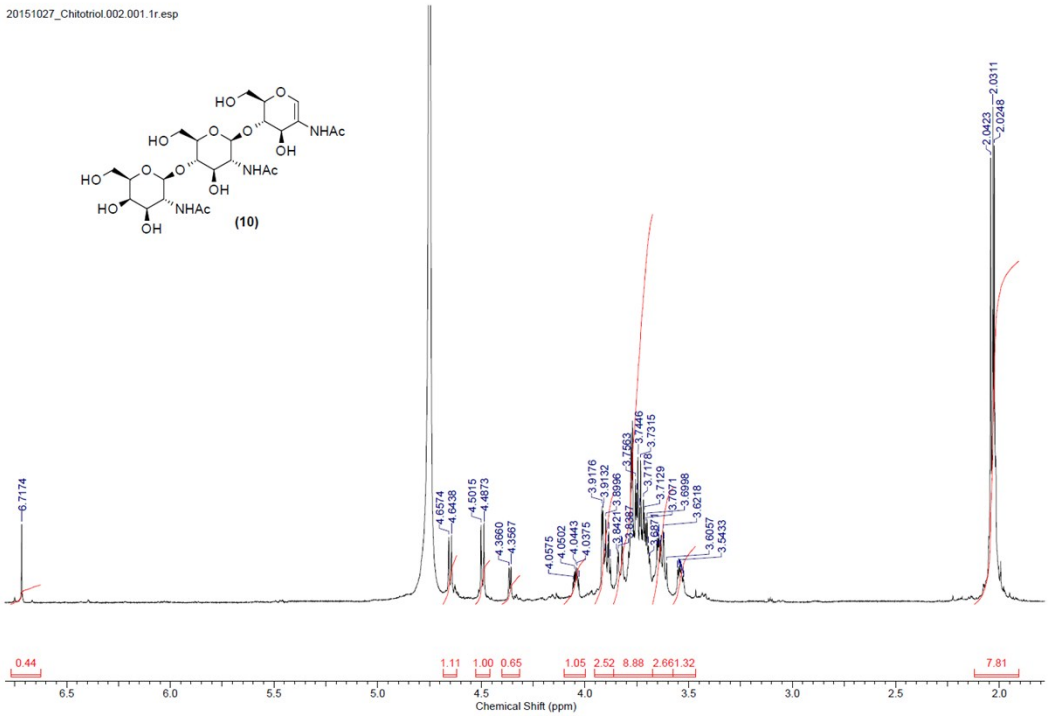
20151027_Chitotriol.002.001.1r.esp
(10)
6.7174
4.6574
4.6438
4.5015
4.4873
4.3660
4.3567
4.0575
4.0502
4.0443
4.0375
3.9176
3.9132
3.8996
3.8421
3.7563
3.7446
3.7315
3.7178
3.7129
3.7071
3.6898
3.6218
3.6057
3.5433
2.0423
2.0311
2.0248
0.44
1.11
1.00
0.65
1.05
2.52
8.88
2.66
1.32
7.81
Chemical Shift (ppm)

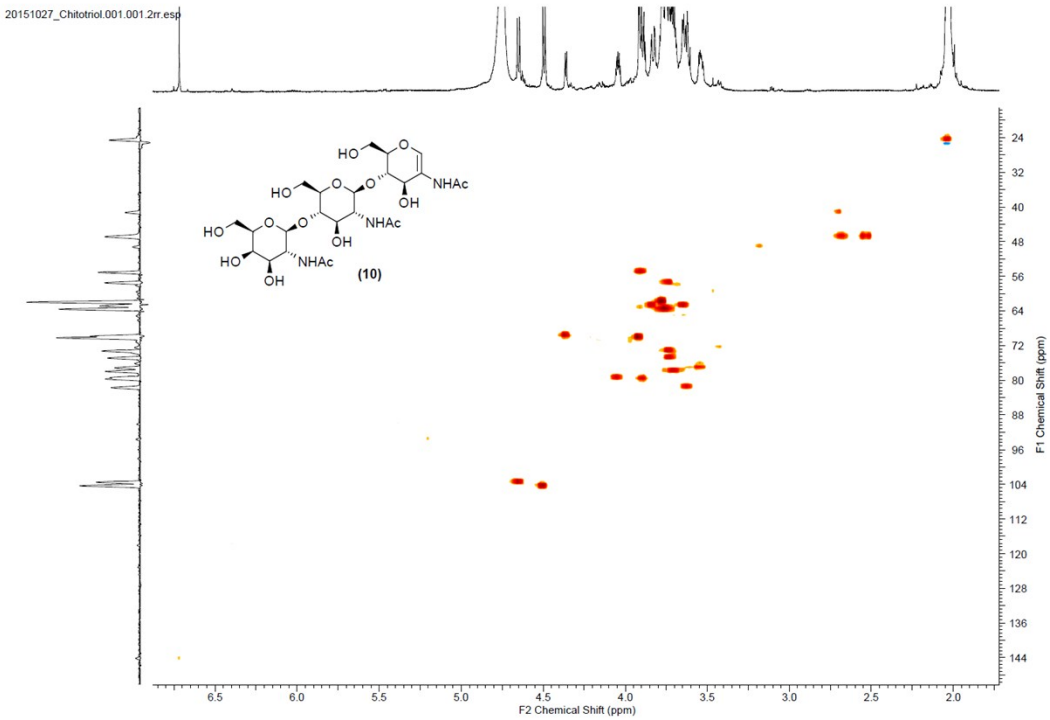
20151027_Chitotriol.001.001.2rr.esp
(10)
F1 Chemical Shift (ppm)
F2 Chemical Shift (ppm)

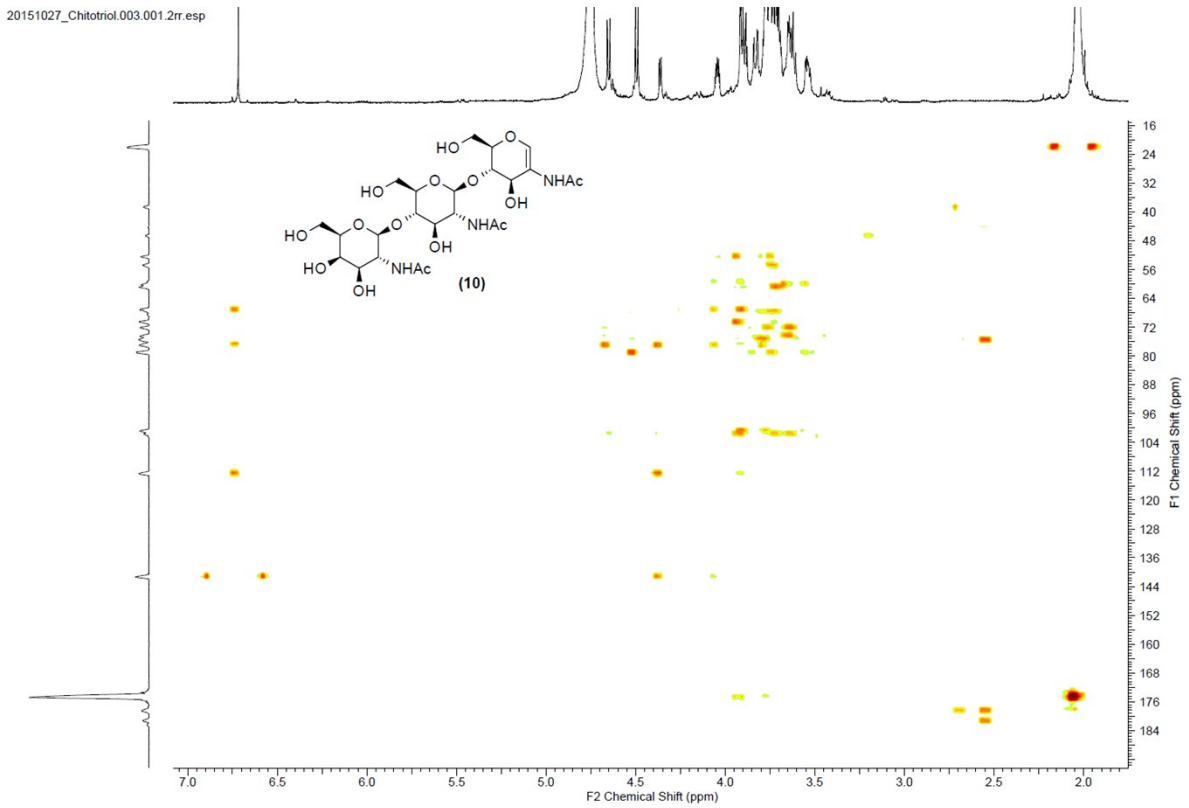
20151027_Chitotriol.003.001.2rr.esp
HO
O
NHAc
OH
HO
O
O
NHAc
OH
HO
O
O
HO
NHAc
OH
(10)
F1 Chemical Shift (ppm)
F2 Chemical Shift (ppm)

**_Sp_Hex expression, purification and crystallization:**

_Sp_Hex was expressed and purified as described previously (1). Crystals were grown at room temperature by the hanging drop vapour diffusion method using equal volumes of reservoir buffer (1.8 M $AmSO_4$, 0.1 M trisodium citrate pH 6) and protein (3.6 mg/ml). Individual _Sp_Hex crystals were soaked for 24 hours with NA-glucal or NTA-glucal at final concentrations of 4 mM to obtain protein-inhibitor complexes. The soaked crystals were cryoprotected in 1.8 M $AmSO_4$, 0.1 M trisodium citrate pH 6, and 25% glycerol prior to flash cooling to 100K for X-ray data collection. X-ray data were collected using a Rigaku R-AXIS IV++ detector and 007HF Microfocus X-ray generator at the University of Manitoba. The X-ray data were indexed using Mosflm (2), then scaled and averaged using SCALA (3). Structures of the _Sp_HEX complex with either NA-glucal or NTA-glucal were determined by molecular replacement using PHASER (from within the PHENIX package (4)) and a structure of _Sp_HEX (PDB ID: 1HP4) (from which solvent molecules had been removed) as a search model. 3D models of NA-glucal and NTA-glucal were constructed using Jligand (5) and restraint files generated using PHENIX eLBOW (4). The Inhibitor models were manually fit into their ascribed electron densities using Coot (6). Refinement of the modeled complexes and addition of solvent was carried out using PHENIX.REFINE (4) and COOT (6). Crystallographic and refinement statistics are presented in Table S1.


1. Mark, B. L., Vocadlo, D. J., Knapp, S., Triggs-Raine, B. L., Withers, S. G., and James, M. N. (2001) Crystallographic evidence for substrate-assisted catalysis in a bacterial beta-hexosaminidase. *J. Biol. Chem.* **276**, 10330–7

2. T.G.G. Battye, L. Kontogiannis, O. Johnson, H.R. Powell and A.G.W. Leslie (2011), IMosflm: a new graphical interface for diffraction-image processing with MOSFLM. Acta Cryst. D67, 271-281.

3. Evans, P. (2006) Scaling and assessment of data quality. *Acta Crystallogr. D. Biol. Crystallogr.* **62**, 72–82

4. Adams, P. D., Afonine, P. V, Bunkóczi, G., Chen, V. B., Davis, I. W., Echols, N., Headd, J. J., Hung, L.-W., Kapral, G. J., Grosse-Kunstleve, R. W., McCoy, A. J., Moriarty, N. W., Oeffner, R., Read, R. J., Richardson, D. C., Richardson, J. S., Terwilliger, T. C., and Zwart, P. H. (2010) PHENIX: a comprehensive Python-based system for macromolecular structure solution. *Acta Crystallogr. D. Biol. Crystallogr.* **66**, 213–221

5. Lebedev, A. A., Young, P., Isupov, M. N., Moroz, O. V, Vagin, A. A., and Murshudov, G. N. (2012) JLigand: a graphical tool for the CCP4 template-restraint library. *Acta Crystallogr. D. Biol. Crystallogr.* **68**, 431–40

6. Emsley, P., and Cowtan, K. (2004) Coot: model-building tools for molecular graphics. *Acta Crystallogr. D. Biol. Crystallogr.* **60**, 2126–2132